

Ultrafast transient-absorption and steady-state fluorescence measurements on 2-aminopurine substituted dinucleotides and 2-aminopurine substituted DNA duplexes

Olaf F. A. Larsen,^{†a} Ivo H. M. van Stokkum,^a Frank L. de Weerd,^a Mikas Vengris,^a Charuvila T. Aravindakumar,^a Rienk van Grondelle,^a Nicholas E. Geacintov^b and Herbert van Amerongen^c

^a Division of Physics and Astronomy, Faculty of Sciences, Vrije Universiteit Amsterdam, De Boelelaan 1081, 1081 HV Amsterdam, The Netherlands

^b Department of Chemistry, New York University, New York, NY 10003

^c Laboratory of Biophysics, Department of Agrotechnology and Food Sciences, Dreijenlaan 3, 6703 HA Wageningen, The Netherlands

Received 30th July 2003, Accepted 3rd November 2003

First published as an Advance Article on the web 20th November 2003

Ultrafast transient-absorption and steady-state fluorescence measurements have been performed on dinucleotides comprising the fluorescent adenine analogue 2-aminopurine and guanine, adenine, cytosine, thymine or hypoxanthine, respectively. Two oligodeoxyribonucleotide duplexes that were site-selectively substituted with a single 2-aminopurine moiety were also studied. A strong quenching of the steady-state fluorescence was observed in all samples. The transient-absorption spectra were remarkably similar to those of the isolated 2-aminopurine (Larsen *et al.*; O. F. A. Larsen, I. H. M. van Stokkum, M.-L. Groot, J. T. M. Kennis, R. van Grondelle and H. van Amerongen, *Chem. Phys. Lett.*, 2003, **371**, 157–163), exhibiting both a fluorescent and a non-fluorescent excited state. There was no evidence for significant amounts of charge-separated states in the transient-absorption spectra. The probability that an excitation of 2AP leads to stable charge transfer products was estimated to be very low ($\sim 0.1\%$). In the systems we studied, the observed fluorescence quenching can largely be explained by a shift of the equilibrium between the two excited states in 2AP, in which the non-fluorescent state is favored.

1. Introduction

The study of charge-transfer processes in DNA is a topic of intense interest.^{1–5} The fluorescent adenine analogue 2-aminopurine (2AP) has often been used to study DNA electron transfer (ET) as well as DNA structural dynamics and heterogeneity.^{1–4,6,7,18–20} The 2AP probe possesses several highly attractive properties. Contrary to the ultrashort excited-state lifetimes of the normal DNA bases, which are typically on the order of hundreds of femtoseconds (fs),^{8,9} the excited-state lifetime of 2AP is relatively long, namely ~ 12 nanoseconds (ns). In aqueous environment (pH = 7) 2AP is highly fluorescent with a quantum-yield of 0.66, and can be selectively excited because of its long wavelength absorption band around 305 nm.^{10,11} Furthermore, 2AP can be incorporated into DNA, replacing a specifically chosen adenine residue for example, without significantly disturbing the B-DNA helix.¹²

Strong quenching of the 2AP fluorescence upon its incorporation into DNA has been attributed to ET processes between the normal DNA bases and the excited 2AP.^{1,4,17,21} Among the normal DNA bases and based on its oxidation potential, guanine (G) is expected to be the most favorable candidate for transferring an electron to an excited 2AP residue. Recently, a structural heterogeneity of the excited state of 2AP has been revealed using ultrafast transient-absorption spectroscopy.¹³ Besides the well-known fluorescent state of 2AP, an additional long-lived non-fluorescent state was also

observed, which was populated to a significant extent after excitation.

Using two-photon ionization of 2AP, ET from nearby guanine moieties to ionized 2AP in DNA was unambiguously demonstrated using transient-absorption techniques.³ In this work, however, we focus on potential ET dynamics between the normal DNA bases and the single-photon excited state of 2AP. Ultrafast transient-absorption as well as steady-state fluorescence techniques have been used. Both single-stranded DNA dinucleotides comprising 2AP and guanine (G), adenine (A), thymine (T), cytosine (C), or inosine (I), respectively, were studied, as were short oligodeoxyribonucleotide duplexes that contained a single 2AP residue. A very strong quenching of the 2AP fluorescence was observed in all of these model systems. However, no evidence for a complete charge-separation due to ET was found. The transient-absorption spectra were highly similar to those of isolated 2AP and did not reveal the spectra of the expected ET products. As in isolated 2AP, in addition to the fluorescent state, a non-fluorescent electronic excited state was present. The observed fluorescence quenching was attributed to an equilibration between these two states, with the non-fluorescent state being present in greater proportion in the DNA system than in isolated 2AP.

2. Experimental

2.1. Chemicals

2AP DNA dinucleotides were obtained from Biolegio (Malden, The Netherlands), with a purity of $\geq 99\%$. The dinucleotides were dissolved in a 20 mM phosphate buffer with

[†] Present address: Institute for Atomic and Molecular Physics (AMOLF), Kruislaan 407, 1098 SJ Amsterdam, The Netherlands; E-mail: o.larsen@amolf.nl

pH = 7.0, containing 100 mM NaCl. Five different dinucleotides were investigated:

5'	2AP – Guanine	3'
5'	2AP – Adenine	3'
5'	2AP – Cytidine	3'
5'	2AP – Thymidine	3'
5'	2AP – Inosine	3'

Synthesis and purification of single-stranded 2AP incorporated DNA oligonucleotides was performed using a Cyclone DNA synthesizer (Biosearch Inc., San Rafael, CA) as described before.³ The required nucleoside phosphoramidites (2AP, G, A, C, and T) and solid supports for DNA synthesis were obtained from Glen Research (Sterling, VA). Two different DNA duplexes were synthesized, both with a single 2AP substitution, as displayed in Fig. 1. The complementary strands, containing no 2AP, were purchased from Biologio (Malden, The Netherlands).

The oligodeoxyribonucleotides were dissolved in the buffer as described above. Hybridization was accomplished by mixing the 2AP-containing strands with their complementary strands, heating for 10 min at 80 °C, and slowly cooling down to room temperature. To ensure that all 2AP-containing strands were hybridized, an excess of 10% of the complementary strand was added. The purity of the duplexes was ~95%. Incorporation of 2AP dramatically reduces the efficiency of the coupling of more bases. The amounts of DNA needed for transient-absorption experiments are much higher than those needed for fluorescence studies. To maximize the synthesis yield, 2AP is placed relatively to the end of each duplex. This may enhance the probability of disruption of base-stacking in the direct vicinity of 2AP, though.

2.2. Steady-state spectroscopy

Absorption measurements were performed on a Perkin Elmer (lambda 40) absorption-spectrophotometer. Polarized steady-state fluorescence emission spectra were measured on a SPF-500 spectrofluorometer (SLM instruments), using an excitation wavelength of 309 nm. At this wavelength, the relative absorbance of the all the normal DNA bases together is very low as compared to the 2AP absorbance (~10%). Isotropic emission spectra were constructed from the parallel and perpendicularly polarized emission spectra according to the literature,²⁴ and used for determination of the amount of fluorescence quenching.

2.3. Transient-absorption spectroscopy

The transient-absorption spectrometer consisted of a 1-kHz Ti:sapphire amplifier and non-collinear optical parametric amplifier (NOPA) system as described in more detail elsewhere.^{13,14} Briefly, fs (pump) excitation-pulses centered at 309 nm were generated by frequency mixing of the 506 nm output of the NOPA with 800 nm pulses. The time evolution of the excited-state dynamics was subsequently monitored using a second white-light (probe) pulse, resulting in an instrument response of ~600 fs FWHM.

5'- AT [2AP] GTT TTA TAA ATC C -3'	"duplex-1"
5'- AT [2AP] AAG TTA TAA ATC C -3'	"duplex-2"

Fig. 1 Sequences of the DNA oligodeoxyribonucleotides with 2AP substitution. The two duplexes were hybridized with their natural complementary strands (not shown), with basepairing according to G-C, A-T and 2AP-T.

With this setup, transient-absorption spectra (absorption difference of the white-light with and without pump pulse) were monitored. Different wavelength intervals were probed (each spanning ~120 nm and all together ranging from ~335 nm to ~520 nm). For duplex-2, a larger wavelength window from ~335 nm to ~690 nm was probed. No significant signal of hydrated electrons from 2AP was observed (2-photon ionization), which are known to be formed when very high excitation densities are used.² Hence, it was assured that primarily one-photon excitation of 2AP was performed and ET from guanine to 2AP radicals could be excluded. All the spectra were recorded at 200 different delay times (the time difference between pump and probe pulses). The time window that was probed was 1 ns for the dinucleotides and "duplex-1", and 5 ns for the "duplex-2" sample. Hence, the precision of "long" ns lifetimes is rather low, and they should merely serve as a first estimate.

3. Data analysis

For each wavelength interval, a typical transient-absorption data set consisted of $> 10^4$ data points (the transient-absorption spectrum was dispersed on 256 pixels, and 200 different delay times were probed). For each sample studied, complete data sets of different wavelength intervals were simultaneously fitted using a sequential global analysis method.^{15,16} In this model, the excited species that is assumed to be present at time zero (more species at time zero are also possible, see below) evolves with a certain decay rate k_1 into another second species, that can subsequently evolve with a slower rate k_2 into a third species, and so on. The last species n obviously decays to its ground state with slowest rate k_n . Each species has its own spectrum, the species associated difference spectrum (SADS) $A_i(\lambda)$. Two different species (1 and 2) are sufficient to describe the transient-absorption datasets of the dinucleotides whereas three lifetimes (and their corresponding SADS) are needed for the duplex-1 and duplex-2 DNA samples. The isotropic decay $I_{\text{iso}}(t)$ is described by:

$$I_{\text{iso}}(t) = \left[\sum_{i=1}^n A_i(\lambda) c_i(t) \right] \otimes I(t) \quad (3.1)$$

With $n = 2$ for the dinucleotides, and $n = 3$ for duplex-1 and -2. $I(t)$ is the instrument response and \otimes denotes convolution. The concentrations c_i are (exponential) functions of k_1 , k_2 , and k_3 . It is important to note that it is not a prerequisite to have only one single species present at time zero. Two species 1 and 2 can also be present at time zero, and in that case k_1 simply represents an equilibration (spectral evolution) between these two states. Hence, structural heterogeneity can be included in this way.

4. Results

4.1. Steady-state fluorescence

The fluorescence of 2AP upon insertion into a dinucleotide or duplex was heavily quenched. The relative fluorescence yields of the different samples studied are summarized in Table 1.

4.2. Transient-absorption spectroscopy

The decay kinetics of all the dinucleotides were simultaneously fitted over the complete wavelength region (335 nm to 520 nm) using the sequential model as described in the data analysis section, using a picosecond (ps) lifetime and a ns lifetime. The kinetic traces arising from duplex-1 could be adequately fitted with three different species absorbing in the UV region (two species with ps lifetimes and one with a ns lifetime). However, not more than two lifetimes could be extracted from

Table 1 Relative fluorescence yields

Molecule	Relative fluorescence yield ($\pm 2 \times 10^{-3}$) ^a
2AP	1
Duplex-1	0.01
Duplex-2	0.02
2AP-G-dinucleotide	0.04
2AP-A-dinucleotide	0.08
2AP-T-dinucleotide	0.09
2AP-C-dinucleotide	0.12
2AP-I-dinucleotide	0.18

^a Determined by the ratios of the areas of the emission spectra of the corresponding molecule and 2AP.

the data in the visible region, and therefore these two wavelength intervals were eventually fitted separately. Duplex-2 displayed three different lifetimes (Table 2) after a simultaneous fit of the complete wavelength window that was probed (335 nm to 690 nm). The SADS of the dinucleotides are shown in Figs. 2a-e, whereas the SADS of duplex-1 and duplex-2 are given in Figs. 3a and 3b respectively. It should be stressed that the displayed spectra with corresponding lifetimes are not the "raw" transient-absorption data, but the results of the global analysis as described in section 3. All the ps lifetimes in Fig. 2 should not be over-interpreted and merely indicate an estimated time-range (30–40 ps in case of the dinucleotides), rather than exact lifetimes. The precision of "long" ns lifetimes should also be treated with care because of the probed time window (see experimental section).

All samples exhibit a very pronounced excited-state absorption spectrum (ESA, positive transient-absorption signal), peaking around 520 nm. The UV region, however, is different for different samples. For the 2AP-G- and 2AP-T-dinucleotide, only ESA seems to be present. For the 2AP-I-, 2AP-A-, and 2AP-C-dinucleotides, a significant increase in the amount of stimulated emission (SE) is observed. SE is reflected by a broad "dip" centered at ~370 nm that is superimposed on the ESA. This SE signal seems to be (almost) absent in the ps component for the 2AP-I- and 2AP-C-dinucleotide, but is clearly present in their ns SADS. For the 2AP-A-dinucleotide, SE can be observed in both the ps and the ns SADS. For duplex-1, the SADS are shown in Fig. 3a. The UV region (see inset) is strikingly similar to the UV region of the 2AP-G-dinucleotide. The 10 ps and 70 ps species show ESA. The ~1 ns component seems somewhat negative, indicating SE. Obviously, a rapid depletion of excited-states has taken place that decreases the ESA signal and makes the SE more clearly observable. The visible region shows again a very pronounced ESA peaking at ~520 nm. For the duplex-2 sample, the complete region from ~335 to ~690 nm was probed. The duplex-2 sample also does show very pronounced ESA for all three species around 520 nm. SE is observed for the 29 ps species. This SE is clearly superimposed on ESA.

Table 2 Isotropic lifetimes τ_F /ps

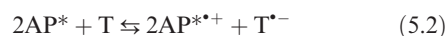
Molecule	τ_1 ($\pm 10\%$)	τ_2 ($\pm 10\%$)	τ_3 ($\pm 10\%$)
duplex 1	10	70	1×10^3
duplex 2	29	2.7×10^2	9.9×10^3
2AP-G	40	4×10^3	—
2AP-A	30	2×10^3	—
2AP-T	40	2×10^3	—
2AP-C	40	1.5×10^3	—
2AP-I	30	1×10^3	—

Derived from the target analysis of the transient-absorption data (see data-analysis section).

5. Discussion

5.1. Steady-state spectroscopy

The fluorescence of 2AP is dramatically quenched in all of the samples studied. Obviously, guanine is not the only residue that can quench the fluorescence of 2AP in DNA; the fluorescence of 2AP is clearly quenched by all of the bases. This is in agreement with earlier results by Fiebig *et al.*,¹⁷ who studied mixtures of 2AP and different DNA bases (although not covalently bound in a dinucleotide system like in our studies). It has been suggested that this quenching of the 2AP fluorescence can be attributed to electron-transfer (ET) processes between excited 2AP (2AP*) and the normal DNA bases.^{1,4,17} Based on the electronic excitation energy of 2AP (3.74 eV), the redox potentials of the normal DNA bases (oxidation potentials for G, A, C, and T respectively 1.29 V, 1.42 V, 1.6 V and 1.7 V vs. NHE¹⁸) and the oxidation potential of 2AP* (1.5 V vs. NHE¹), the free Gibbs energy for such an ET reaction can be estimated using the Rehm-Weller equations.²⁵ Based on this estimation, oxidation of guanine by 2AP* (eqn. (5.1)) is expected to be the most favorable ET reaction, whereas oxidation of thymine by 2AP* is expected to be the least favorable. Alternatively, reduction of thymine by 2AP* (eqn. (5.2)) could take place.



Hypoxanthine should, in principle, possess little driving force for a charge-transfer reaction with 2AP*, based on its redox potential of 1.5 V vs. NHE.¹ It is important to note that the (unknown) activation energies for such ET reactions can, of course, influence the probabilities of these reactions to take place. Furthermore, the redox potentials of the individual bases^{1,18} may be altered upon incorporation into DNA. The amount of quenching for the systems we studied seems to scale with the redox potential of the base that is linked to the 2AP residue. Less driving force for oxidation of the linked base results in less fluorescence quenching ($G < A < I$), and less driving force for reduction of the linked base also results in less fluorescence quenching ($T < C < I$). The observed quenching can, however, most likely not be explained by a redox reaction only, because the fluorescence of the 2AP-I-dinucleotide is also significantly quenched (82%). Similar conclusions were drawn in a previous study.⁶ This, together with the aforementioned considerations, points out that detailed speculations are not warranted. However, based on our results it seems likely that the observed fluorescence quenching of 2AP has at least partly a charge-transfer process at its base.

5.2. Transient-absorption spectroscopy

Excited-state heterogeneity. Recently, transient-absorption spectra of excited 2AP molecules have been reported.¹³ These data revealed that even in the case of the free 2AP molecule, a heterogeneity of excited-states of 2AP is observable. Two electronic states were shown to be populated after excitation at 309 nm. One state is fluorescent (resulting in a negative signal in the UV due to stimulated emission, SE), whereas the second one is long-lived (> 15 ns), though non-fluorescent (resulting in positive signal in the UV transient-absorption spectrum due to excited-state absorption, ESA). Pronounced ESA was observed around 520 nm for both states. The transient-absorption spectra measured for the dinucleotides and DNA duplexes are quite similar to those of the isolated 2AP molecules. All samples exhibit a very pronounced ESA for all species peaking around 520 nm. However, the ESA spectrum in the UV region seems to be dependent on the base that is adjacent to 2AP in the dinucleotides and probably reflects a specific interaction between the two bases. In the case of the 2AP-G-dinucleotide, only ESA is observed in the UV region and there

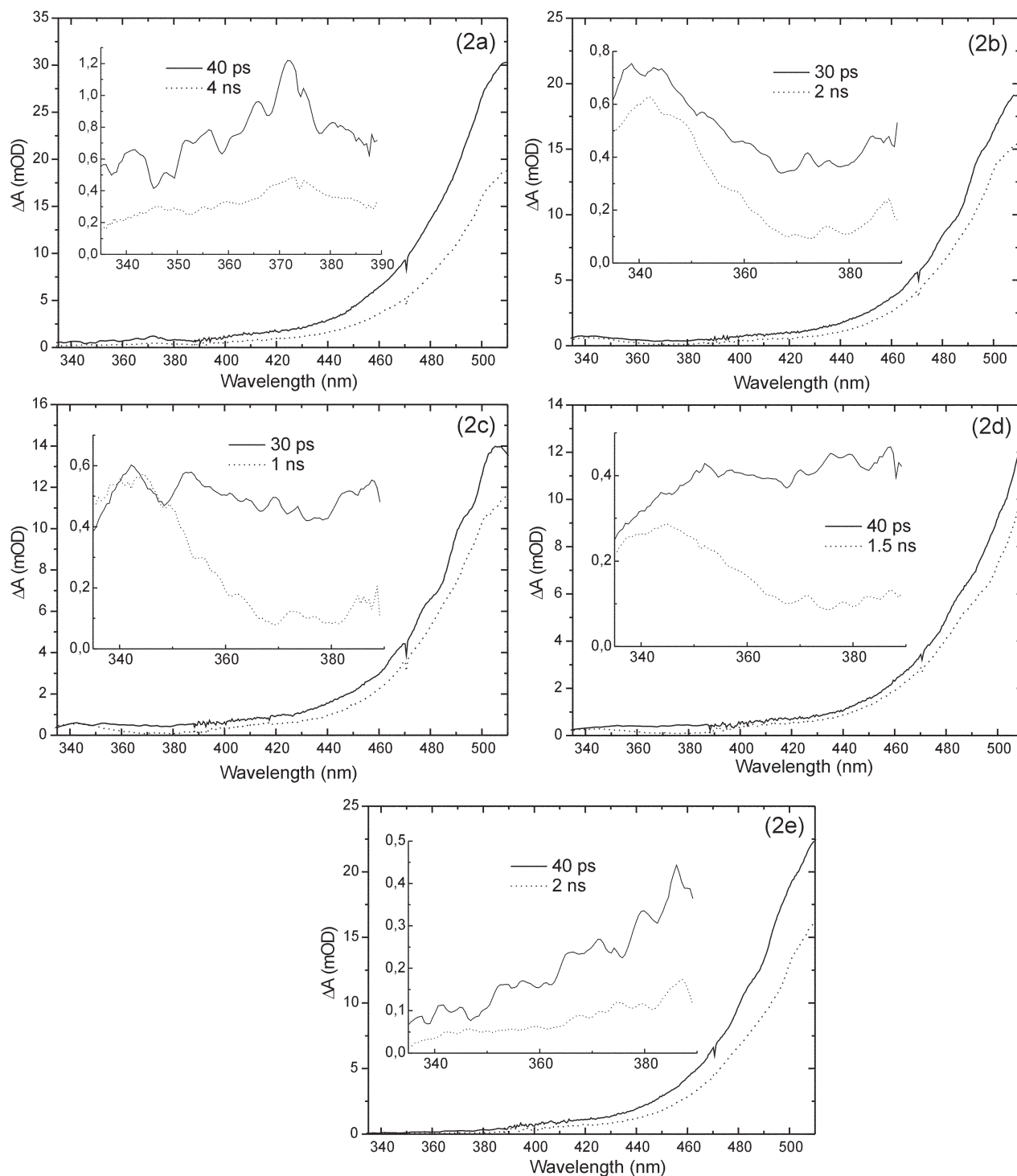


Fig. 2 SADS of the 2AP-dinucleotides obtained from global analysis of the transient-absorption data. The insets show the UV region from 335 nm to 390 nm. (a) 2AP-G, (b) 2AP-A, (c) 2AP-I, (d) 2AP-C, (e) 2AP-T.

is no significant SE. This is to be expected considering the dramatic quenching of the steady state fluorescence. For the 2AP-T-dinucleotide, no SE can be observed either. However, significant steady-state fluorescence is still observed (9%). In the case of the other dinucleotides, a significant (30–40 ps) risetime in the SE can be observed. The amount of SE seems in line with the observed steady-state quenching. Besides the 30–40 ps risetime, a strong decrease in the total transient-absorption signal is also clearly observed on the ps timescale in all samples. Hence, it seems that a rapid depopulation of excited states takes place.

The transient-absorption spectrum in the UV region of duplex-1 is very similar to that of the 2AP-G-dinucleotide as

well as to that of the 2AP-T-dinucleotide (all exhibit predominantly ESA and very little SE), which is not surprising considering that in this sample the 2AP residue is flanked by G and T. In the case of duplex-2, a significant SE signal is present in the first spectrum but disappears on a ~ 30 ps time scale (no SE can be seen in the 272 ps and ~ 10 ns spectra). This is in contrast to the 2AP-A-dinucleotide, where SE is still present after 30 ps (reflected in the broad negative dip in the 2 ns spectrum).

In the following discussion, we will first focus on the dinucleotide data, because these systems are relatively easier to model than the duplex data. If one assumes just one (fluorescent) species to be present in the dinucleotide, one can calculate that the expected lifetime of this species does not match

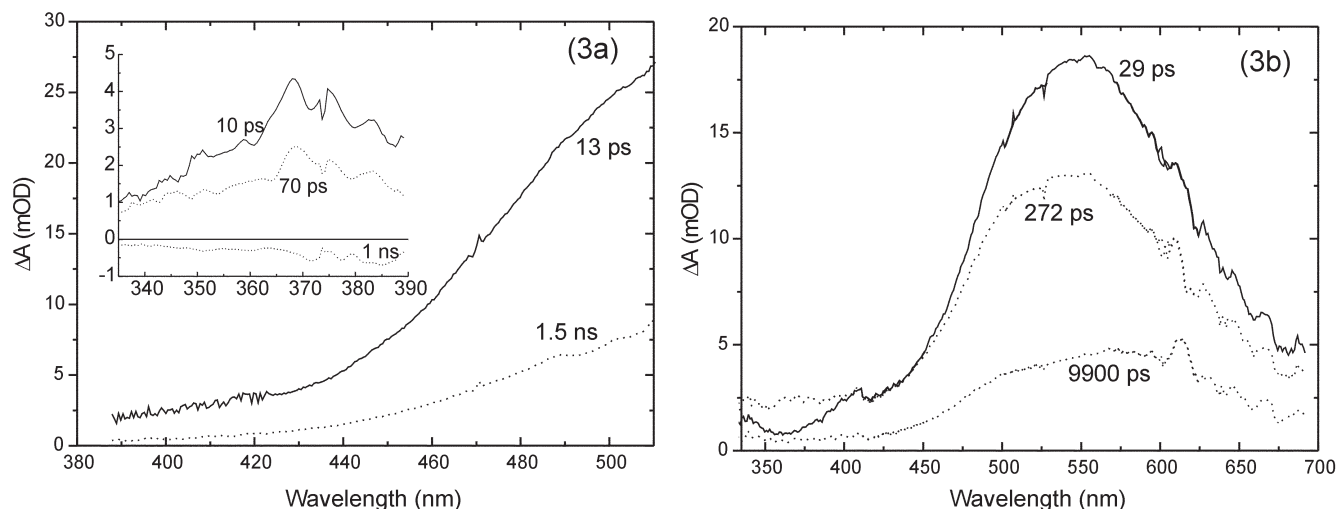


Fig. 3 SADS of the DNA duplexes obtained from global analysis of the transient-absorption data. (a) duplex-1 (the inset shows the UV-region), (b) duplex-2.

with the experimental data. The extent of quenching of the steady-state fluorescence of, for example, the 2AP-G-dinucleotide is 96%. In a dynamic quenching model this would correspond to a reduction of the original 2AP lifetime of 11.8 ns¹⁸ to ~500 ps (4% of 11.8 ns). However, the measured transient-absorbance lifetimes are 30–40 ps and 1–4 ns respectively. A model in which only one fluorescent state is present can thus be rejected in the case of the 2AP-G-dinucleotide. Furthermore, it is not possible to model the 2AP-G-dinucleotide using only one non-fluorescent non-radiative state either, because some steady-state fluorescence is observed. Thus, coexisting states are needed to adequately describe the data. The 2AP-G-dinucleotide data can be most simply modelled using a minimum of two different excited states. Besides a fluorescent state, a non-radiative state must be present as well in order to account for the ensemble of observations. Similar arguments hold for the other dinucleotides. Based on our observations, the scheme shown in Fig. 4 is proposed to explain both the steady-state emission and the transient-absorption data for all the dinucleotides. This scheme is analogous to that proposed for isolated 2AP, except that a clear 30–40 ps equilibration time was observed in the case of the dinucleotides.¹³

In this scheme, structural heterogeneity of the 2AP moiety is assumed to exist in the ground state, resulting in two different populations of 2AP. This heterogeneity can arise from differences in the relative configurations of the two bases in the dinucleotides involving, for example, different extents of base-stacking interactions. Upon excitation, the interactions between the two bases are altered, resulting in a re-adjustment of the orientations of the two bases relative to one another. Our observations are consistent with a two-state model, in which one of these states decays predominantly by non-radiative pathways, and the other by a partially radiative pathway. Following photoexcitation on the fs time scale, an equilibration between these two types of excited states occurs within the first 30–40 ps, which is reflected in the observed 30–40 ps risetime in SE in the 2AP-A-, -C-, and -I-dinucleotides. The depopulation of excited states taking place within this 30–40 ps is also monitored. This results in less ESA and can be observed most clearly in the case of the 2AP-G- and 2AP-T-dinucleotides, by comparing the intensity of the ESA signal at ~520 nm (see Figs. 2a and 2e). The other dinucleotides exhibit this depopulation as well, although it is less pronounced. Obviously, this loss of ESA is still not sufficient to clearly observe the SE signals in the 2AP-G- and 2AP-T-dinucleotides. The observed ns lifetime state must be a combination of both a fluorescent state and a non-radiative state, but the

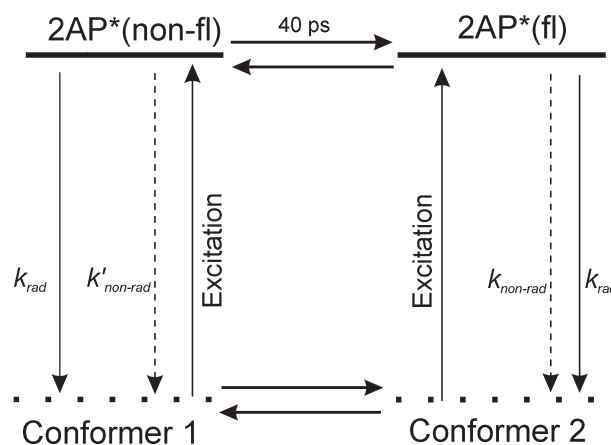


Fig. 4 Proposed minimal reaction scheme of an excited 2AP moiety in a dinucleotide. In the ground state, two conformers (1 and 2) are in equilibrium with one another with interconversion from one to the other being negligibly slow on the time scale of excitation. In the excited state, equilibration between the two states takes place on a time scale of ~40 ps. Both states decay by both radiative (k_{rad}) and non-radiative ($k_{\text{non-rad}}$ or $k'_{\text{non-rad}}$) pathways. However, the fluorescence quantum yield is significantly higher for the 2AP*(fl) state (although $k_{\text{non-rad}} > k_{\text{rad}}$), whereas in the non-radiative state 2AP*(non-fl), $k'_{\text{non-rad}} \gg k_{\text{rad}}$ (see text). Solid lines: radiative transitions, dashed lines: non-radiative transitions.

two states cannot be resolved within the limitations of the current signal-to-noise ratio. The observed ns lifetime (with corresponding rate k_{slow}) contains both the decay rates of the fluorescent state (k_{rad} and $k_{\text{non-rad}}$) and the decay rates of the non-radiative state (k_{rad} and $k'_{\text{non-rad}}$) according to $k_{\text{slow}} = x*(k_{\text{rad}} + k_{\text{non-rad}}) + y*(k_{\text{rad}} + k'_{\text{non-rad}})$, x and y being the contributions of the fluorescent channel and the non-radiative channel to the observed ns lifetime excited state. Hence, analogous to isolated 2AP,¹³ both a fluorescent and a non-radiative state are present. However, contrary to isolated 2AP, a clear equilibration on a timescale of 30–40 ps between these two states is observed in the case of the dinucleotides. It is important to note that both states can decay both radiatively as well as non-radiatively. However, for the non-radiative state, k_{rad} is much smaller than the non-radiative rate: $k_{\text{rad}} \ll k'_{\text{non-rad}}$. For the radiative state, on the other hand, this difference is less dramatic: $k_{\text{rad}} < k_{\text{non-rad}}$. In the radiative state, $k_{\text{non-rad}}$ must still be much larger than k_{rad} since the

fluorescence lifetime is much less than 10 ns, but the difference in rates is less pronounced than for the non-radiative state.

For the DNA-duplexes, a minimum of three different excited states is observed. These states are, analogous to the dinucleotides, also attributed to co-existing fluorescent and non-fluorescent states. For duplex-1, lifetimes of ~ 10 ps, ~ 70 ps and ~ 1 ns were extracted from the transient-absorption spectra in the UV region, whereas only two lifetimes (~ 13 ps and 1.5 ns) were needed to fit the data in the visible region (Fig. 3a). The ns species exhibits a small amount of fluorescence. Also for this duplex, a rapid depopulation of excited states is observed.

For duplex-2, three different species can be extracted from the data. Two non-radiative states are present, decaying with characteristic lifetimes of respectively ~ 270 ps and ~ 10 ns. Only one fluorescent state is observed (29 ps). The fluorescence can clearly be observed at ~ 370 nm, represented by the “dip” in the ESA centered around this wavelength (Fig. 3b). The fluorescence cannot originate only from this state, because the yield calculated from this lifetime is lower than that measured in steady-state fluorescence measurements. A fluorescence component that decays with a ~ 30 ps lifetime would give rise to a quenching of almost 100% (~ 30 ps is 0.3% of 11.8 ns, the original lifetime of 2AP, hence a quenching of 99.7% is expected). However, the observed steady-state quenching is 98%. Hence, the spectra of the two other non-radiative states (272 ps and ~ 10 ns) also contain some stimulated emission (SE) originating from either unresolved states, or from $k'_{\text{non-rad}}$ being somewhat smaller as compared to $k_{\text{non-rad}}$ from the other samples. Nevertheless, since the fluorescence contributions are still very small, we also call these states “non-radiative”. No equilibration between the different states is observed as in the dinucleotide samples and no rise in fluorescence could be detected. Possibly, the fluorescent state in this duplex can interact to a lesser extent with the other states due to a high-energy barrier. Contrary to the dinucleotide samples, more than two lifetimes are observed in the DNA samples. These lifetimes can be attributed to different conformations of the DNA molecules that require different reorientation times before they are rapidly depopulated (“quenching” of both fluorescent and non-radiative states) analogous to earlier results.⁶

Summarizing, two different electronic excited states are populated when 2AP is incorporated into a substituted DNA molecule: a fluorescent state and a non-fluorescent state. These states are analogous to the fluorescent and the non-radiative state in isolated 2AP.¹³ In the case of 2AP in DNA, the equilibrium between these two states is clearly shifted to the non-fluorescent state as compared to isolated 2AP, thus accounting for the steady-state fluorescence quenching. This can be observed in the transient-absorption data in the case of the 2AP-G-dinucleotide, 2AP-T-dinucleotide, and duplex-1 (predominantly ESA, originating from the non-fluorescent state, in the UV region). For the other samples, the equilibrium is shifted somewhat more in favor of the fluorescent state, although the non-fluorescent state is still the dominant species (reflected by the high ESA “background” in the UV region of the transient-absorption spectrum, on which the SE of the fluorescent state is superimposed).

One-photon induced electron transfer? Electron transfer (ET) resulting in stable, long-living, charge-separated species does at most take place with low probability. This is illustrated by the relatively low amounts of permanent products that were observed. These products were determined by comparing the steady-state absorption spectrum before and after the transient-absorption experiments on the studied samples, which were shown to be 7% at the highest (data not shown). Based on the expected bleaching of the 2AP absorption band at 309 nm (~ 5 mOD for each lasershot,

Appendix 1), and the observed permanent product at 309 nm, the probability of permanent product formation upon excitation was estimated to be $\sim 0.1\%$ for the 2AP-G-dinucleotide (see Appendix 1).

If ET indeed occurs upon one-photon excitation of 2AP, the corresponding product species should be revealed via their transient-absorption spectra. Because ET from G to 2AP* has been reported,^{1,4,17} and because G in DNA is the most likely species to undergo an ET reaction, we focus our discussion first on the 2AP-G-dinucleotide. In the case of ET, the transient-absorption spectrum is expected to be a sum of the absorption spectra of G^{*+} and $2AP^{*+-}$, according to eqn. 5.1. To our knowledge, the absorption spectrum of $2AP^{*+-}$ has never been measured. In our experiments, low white-light signal prevents us from measuring transient-absorption signals at 310 nm. At this wavelength, a characteristic absorption band for G^{*+} should be present in case of ET. However, based on the spectrum of G^{*+} ,²² at ~ 380 nm a significant transient-absorption signal of G^{*+} should also be present in the case of ET. The estimated transient-absorption signal around 380 nm should be ~ 2.4 mOD (see Appendix 2) if one assumes 96% ET efficiency (to explain the fact that for the 2AP-G-dinucleotide 96% of the fluorescence is quenched). The transient-absorption signal we observe at ~ 380 nm is ~ 0.5 mOD, suggesting that little absorption of G^{*+} is observed. Thus, the observed signal is at least a factor of 5 too small to be ascribed to G^{*+} . Another argument that argues against oxidation of the guanine moiety by 2AP* is the fact that the transient-absorption spectrum in the visible region looks remarkably similar to that of the isolated 2AP base (see ref. 13), which would be surprising in the case of the formation of ET products. Analogous to earlier reports on benzo[a]pyrenetetraol-nucleoside complexes²³ and our steady-state emission data, it seems that a fast charge-separation (possibly coupled to a proton-transfer reaction) indeed takes place, but is followed by a rapid recombination. This rapid recombination would prevent observation of the charge-separated states. Similar arguments can be made for the DNA duplexes; no spectral features from G^{*+} resulting from ET could be observed.

In summary, our steady-state fluorescence results indicate that a charge-transfer process is most likely at the base of the observed steady-state quenching because the fluorescence seems to scale with the redox potential of the base flanking the 2AP moiety. However, within the limits of our time-resolution and signal-to-noise ratio, fast ET from guanine to 2AP* resulting in stable ions occurs at most with low probability because no product-spectra could be determined. A very rapid recombination after charge separation may account for the absence of these spectra. In 2AP-substituted DNA, the non-fluorescent excited-state of 2AP is more favored as compared to isolated 2AP, which explains the steady-state fluorescence quenching to a large extent. Future experiments in which the degree of charge separation can be investigated in more detail, as in (time-resolved) Stark spectroscopy, will be performed.

Appendix 1. Expected formation of product

In this appendix, the probability of charge transfer upon excitation of 2AP is calculated by combining the expected bleaching of the 2AP band in the transient absorption experiments with the observed permanent product formation. The bleaching is calculated as follows. The excitation power used at 309 nm is 300 mW at 1 kHz, giving 3×10^{-7} J pulse⁻¹, corresponding to 4.7×10^{11} photons per pulse. The absorption of the sample at 309 nm is 0.2 mm⁻¹. Hence, the number of excited molecules can be calculated: $OD = 0.2 \text{ mm}^{-1} = -\log(I/I_0) = -\log(I/4.7 \times 10^{11})$, hence $I = 3 \times 10^{11}$ photons are transmitted. The difference is the amount of absorbed photons: $4.7 \times 10^{11} - 3 \times 10^{11} = 1.7 \times 10^{11}$ photons are absorbed, hence

also 1.7×10^{11} excited molecules. The probing volume is about 3.14×10^{-8} l, which results in a concentration of excited 2AP molecules, 2AP*, of 9×10^{-6} M. Using $\epsilon = 5400$,¹¹ we expect a bleaching of: OD = $5400 \times 4.9 \times 10^{-5}$ M \times 0.1 = 5 mOD at 310 nm. To obtain the transient absorption signal, 9.6×10^6 lasershots were used. The expected bleach of 2AP is 5 mOD per shot, so one expect 4.8×10^4 OD units bleaching if all the excited molecules were confined in the probing volume. The probing volume is $\sim 3.14 \times 10^{-8}$ l. The total volume of the sample ~ 0.1 cm \times 1.5 cm \times 1 cm = 0.15×10^{-3} l. Hence the volume ratio is 4.8×10^3 and the expected bleaching signal in the cuvet is 4.8×10^4 OD/ 4.8×10^3 = 10 OD units. The typical amount of steady-state product (difference steady-state absorption spectrum after and before transient-absorption measurement) at 309 nm is ~ 0.01 OD unit. Hence, the probability that an excitation of 2AP leads to charge transfer is $\sim 0.1\%$. Of course, this calculation is based on the expectation that significant mixing of the bleached molecules with the molecules outside the probing volume takes place, due to diffusion or convection. If this would not be the case, all the bleached molecules would stay confined in the very small probing volume, resulting in a much smaller amount of steady-state product absorption signal.

Appendix 2. Expected signal of electron transfer products

In this appendix we will consider the electron transfer (ET) reaction between 2AP* and G according to eqn. (5.1), because this is in general to be considered the most likely candidate for ET to occur upon excitation of 2AP. The concentration of 2AP*⁻ is in appendix 1 calculated to be 9×10^{-6} M. If we assume that quenching occurs because 96% of the 2AP* is indeed converted into 2AP*⁻ (the quenching of the steady-state fluorescence is 96%), the concentration of G^{•+} is 96% of 9×10^{-6} M = 8.6×10^{-6} M. The expected OD signal at 380 nm due to G^{•+} cations is thus: OD = 8.6×10^{-6} M \times 2720 \times 0.1 = 2.4 mOD (using $\epsilon = 2720$ from ref. 21).

Acknowledgements

Dr V. Y. Shafirovich is gratefully acknowledged for technical support and fruitful discussions. Dr Aravindakumar acknowledges the financial support (B 81-705) from the Netherlands Organisation for Scientific Research (NWO).

References

- 1 S. O. Kelley and J. K. Barton, *Science*, 1999, **283**, 375–381.
- 2 V. Shafirovich, A. Dourandin, W. Huang, N. P. Luneva and N. E. Geacintov, *J. Phys. Chem. B*, 1999, **103**, 10924–10933.
- 3 V. Shafirovich, A. Dourandin, W. Huang, N. P. Luneva and N. E. Geacintov, *Phys. Chem. Chem. Phys.*, 2000, **2**, 4399–4408.
- 4 C. Wan, T. Fiebig, S. O. Kelley, C. R. Treadway, J. K. Barton and A. H. Zewail, *Proc. Natl. Acad. Sci. USA*, 1999, **96**, 6014–6019.
- 5 F. D. Lewis, X. Liu, J. Liu, S. E. Miller, R. T. Hayes and M. R. Wasielewski, *Nature*, 2000, **406**, 51–53.
- 6 O. F. A. Larsen, I. H. M. van Stokkum, B. Gobets, R. van Grondelle and H. van Amerongen, *Biophys. J.*, 2001, **81**, 1115–1126.
- 7 T. M. Nordlund, D. Xu and K. O. Evans, *Biochemistry*, 1993, **32**, 12090–12095.
- 8 J.-M. L. Pecourt, J. Peon and B. Kohler, *J. Am. Chem. Soc.*, 2001, **123**, 10370–10378.
- 9 T. Gustavsson, A. Sharonov, D. Onidas and D. Markovitsi, *Chem. Phys. Lett.*, 2002, **356**, 49–54.
- 10 D. C. Ward, E. Reich and L. Stryer, *J. Biol. Chem.*, 1969, **244**, 1228–1237.
- 11 A. Holmén, B. Nordén and B. Albinsson, *J. Am. Chem. Soc.*, 1997, **119**, 3114–3121.
- 12 L. C. Sowers, G. V. Fazakerley, R. Eritja, B. E. Kaplan and M. F. Goodman, *Proc. Natl. Acad. Sci. USA*, 1986, **83**, 5434–5438.
- 13 O. F. A. Larsen, I. H. M. van Stokkum, M.-L. Groot, J. T. M. Kennis, R. van Grondelle and H. van Amerongen, *Chem. Phys. Lett.*, 2003, **371**, 157–163.
- 14 C. C. Gradinaru, I. H. M. van Stokkum, A. A. Pascal, R. van Grondelle and H. van Amerongen, *J. Phys. Chem. B*, 2000, **104**, 9330–9342.
- 15 I. H. M. van Stokkum, T. Scherer, A. M. Brouwer and J. W. Verhoeven, *J. Phys. Chem.*, 1994, **98**, 852–866.
- 16 A. R. Holzwarth, in *Biophysical Techniques in Photosynthesis*, eds. J. Ames and J. Hoff, Kluwer Academic Publishers, Dordrecht, 1996, p. 75–92.
- 17 T. Fiebig, C. Z. Wan and A. H. Zewail, *Chem. Phys. Chem.*, 2002, **3**, 781–788.
- 18 S. Steenken and S. V. Jovanovic, *J. Am. Chem. Soc.*, 1997, **119**, 617–618.
- 19 C. R. Guest, R. A. Hochstrasser, L. C. Sowers and D. P. Millar, *Biochemistry*, 1991, **30**, 3271–3279.
- 20 R. A. Hochstrasser, T. E. Carver, L. C. Sowers and D. P. Millar, *Biochemistry*, 1994, **33**, 11971–11979.
- 21 C. Wan, T. Fiebig, O. Schiemann, J. K. Barton and A. H. Zewail, *Proc. Natl. Acad. Sci. USA*, 2000, **97**, 14052–14055.
- 22 L. P. Candéias and S. Steenken, *J. Am. Chem. Soc.*, 1989, **111**, 1094–1099.
- 23 V. Y. Shafirovich, S. H. Courtney, N. Ya and N. E. Geacintov, *J. Am. Chem. Soc.*, 1995, **117**, 4920–4929.
- 24 H. van Amerongen and W. S. Struve, *Meth. Enzymol.*, 1995, **246**, 259–283.
- 25 D. Rehm and A. Weller, *Isr. J. Chem.*, 1970, **8**, 259–271.